

Electrothermal feedback in superconducting nanowire single-photon detectors

Andrew J. Kerman,¹ Joel K.W. Yang,² Richard J. Molnar,¹ Eric A. Dauler,^{1,2} and Karl K. Berggren²

¹*Lincoln Laboratory, Massachusetts Institute of Technology, Lexington, MA, 02420*

²*Research Laboratory of Electronics, Massachusetts Institute of Technology, Cambridge, MA, 02139*

(Dated: October 24, 2018)

We investigate the role of electrothermal feedback in the operation of superconducting nanowire single-photon detectors (SNSPDs). It is found that the desired mode of operation for SNSPDs is only achieved if this feedback is unstable, which happens naturally through the slow electrical response associated with their relatively large kinetic inductance. If this response is sped up in an effort to increase the device count rate, the electrothermal feedback becomes stable and results in an effect known as latching, where the device is locked in a resistive state and can no longer detect photons. We present a set of experiments which elucidate this effect, and a simple model which quantitatively explains the results.

PACS numbers: 74.76.Db, 85.25.-j

Superconducting nanowire single-photon detectors (SNSPDs) [1, 2, 3, 4] have a combination of attributes found in no other photon counter, including high speed, high detection efficiency over a wide range of wavelengths, and low dark counts. Of particular importance is their high *single-photon* timing resolution of ~ 30 ps [4], which permits extremely high data rates in communications applications [5, 6]. Full use of this electrical bandwidth is limited, however, by the fact that the maximum count rates of these devices are much smaller (a few hundred MHz for $10 \mu\text{m}^2$ active area, and decreasing as the area is increased [2]), limited by their large kinetic inductance and the input impedance of the read-out circuit [2, 7]. To increase the count rate, therefore, one must either reduce the kinetic inductance (by using a smaller active area or through the use of different materials or substrates) or increase the load impedance [7]. However, either one of these approaches causes the wire to “latch” into a stable resistive state where it no longer detects photons [8]. This effect arises when negative electrothermal feedback, which in normal operation allows the device to reset itself, is made fast enough that it becomes stable. We present experiments which probe the stability of this feedback, and we develop a model which quantitatively explains our observations.

The operation of an SNSPD is illustrated in Fig. 1(a). A nanowire (typically $\sim 100\text{nm}$ wide, 5nm thick) is biased with a DC current I_0 near the critical current I_c . When a photon is absorbed, a short (< 100 nm long) normal domain is nucleated, giving the wire a resistance $R_n(t)$; this results in Joule heating which causes the normal domain (and consequently, R_n) to expand in time exponentially. The expansion is counteracted by negative electrothermal feedback associated with the load R_L (typically a 50Ω transmission line), which forms a current divider with the nanowire and tends to divert current out of it, thereby reducing the heating (and producing a voltage across the load). In a correctly functioning device, this feedback is sufficiently slow so that it is unstable: that is, the inductive time constant is long enough so that before appreciable current is diverted out of the load, Joule heating has

already caused the normal domain to grow large enough so that $R_n \gg R_L$ [11]. The current in the device then drops nearly to zero, allowing it to quickly cool down and return to the superconducting state, after which the current recovers with a time constant $\tau_e \equiv L/R_L$ [2]. If one attempts to shorten τ_e , at some point the negative feedback becomes fast enough to counterbalance the fast Joule heating before it runs away, resulting in a stable resistive domain, known as a self-heating hotspot [9].

In a standard treatment of these hotspots [9], solutions to a one-dimensional heat equation are found in which a normal-superconducting (NS) boundary propagates at constant velocity v_{ns} , for fixed device current I_d [9, 10]. This results in a solution of the form:

$$v_{ns} = v_0 \frac{\alpha(I_d/I_c)^2 - 2}{\sqrt{\alpha(I_d/I_c)^2 - 1}} \approx \frac{1}{\gamma} (I_d^2 - I_{ss}^2) \quad (1)$$

where $v_0 \equiv \sqrt{A_{cs}\kappa h}/c$ is a characteristic velocity (A_{cs} is the wire’s cross-sectional area, κ is its thermal conductivity, and c and h are the heat capacity and heat transfer coefficient to the substrate, per unit length, respectively), I_c is the critical current, and $\alpha \equiv \rho_n I_c^2 / h(T_c - T_0)$ is known as the Stekly parameter (ρ_n is the normal resistance of the wire per unit length, T_0 and T_c are the substrate and superconducting critical temperatures) which characterizes the ratio of joule heating to conduction cooling in the normal state [9]. Equation 1 is valid when $T_0 \ll T_c$, and the approximate equality holds for small deviations $\delta I \equiv I - I_{ss}$, with $\gamma \equiv (T_c - T_0)(c/\rho_n)\sqrt{h/\kappa A_{cs}}$ and $I_{ss}^2 \equiv 2h(T_c - T_0)/\rho_n$. The physical meaning of eq. 1 is clear: the NS boundary is stationary only if the local power density is equal to a fixed value; if it is greater, the hotspot will expand ($v_{ns} > 0$), if less it will contract ($v_{ns} < 0$).

We can use eq. 1 to describe the electrothermal circuit in fig. 1(a), by combining it with: $dR_n/dt = 2\rho_n v_{ns}$ and $I_d R_n + L dI_d/dt = R_L(I_0 - I_d)$. Assuming that the small-signal stability of the DC hotspot solution ($I_d = I_{ss}$, $R_{ss} = R_L(I_0/I_{ss} - 1)$) determines whether it will

latch, we linearize about this solution to obtain a second-order system, with damping coefficient $\zeta = \frac{I_0}{4I_{ss}} \sqrt{\tau_{th}/\tau_e}$, where $\tau_{th} \equiv R_L/2\rho_n v_0$ is a thermal time constant. This can be re-expressed as $\zeta = \frac{1}{4} \sqrt{\tau_{th,tot}/\tau_{e,tot}}$, with $\tau_{e,tot} \equiv L/R_{tot}$ and $\tau_{th,tot} \equiv R_{tot}/2\rho_n v_0$, where $R_{tot} \equiv R_L + R_{ss}$. If the damping is less than some critical, minimum value ζ_{latch} , the feedback cannot stabilize the hotspot during the initial photoresponse, as described above, and the device operates normally. However, since the steady-state solution gives $R_{ss} \propto I_0$ (as I_0 is increased, a larger hotspot is necessary for $I_d = I_{ss}$) the hotspot becomes more stable as I_0 is increased, until eventually $\zeta(I_{latch}) = \zeta_{latch}$ and the device latches. For a correctly functioning device, $I_{latch} > I_c$, so that latching does not affect its operation. However, if τ_e is decreased, I_{latch} decreases, and eventually it becomes less than I_c . This prevents the device from being biased near I_c [17], resulting in a drastic reduction in performance [12, 13].

Devices used in this work were fabricated from ~ 5 nm thick NbN films, deposited on R-plane sapphire substrates in a UHV DC magnetron sputtering system (base pressure $< 10^{-10}$ mbar). Film deposition was performed at a wafer temperature of ~ 800 C and a pressure of $\sim 10^{-8}$ mbar [15]. Aligned photolithography and liftoff were used to pattern ~ 100 nm thick Ti films for on-chip resistors [8], and Ti:Au contact pads. Patterning of the NbN was then performed with e-beam lithography using HSQ resist [3]. Devices were tested in a cryogenic probing station at temperatures of 1.8-12K using the techniques described in Refs. [2, 3].

Figure 1(c)-(f) show data for a set of ($3\mu\text{m} \times 3.3\mu\text{m}$ active area) devices having various resistors R_S in series with the 50Ω readout line [8] [fig. 1(b)] so that $R_L = 50\Omega + R_S$. Panels (c) and (d) show averaged pulse shapes for devices with $R_S = 0$ and $R_S = 250\Omega$, respectively. Clearly, the reset time can be reduced; however, this comes at a price. Panels (e) and (f) show, for devices with different R_S , the current $I_{switch} \equiv \min(I_c, I_{latch})$ above which each device no longer detects photons, and the measured detection efficiency (DE) at $I_0 = 0.975 I_{switch}$ [17]. The data are plotted vs. the speedup of the reset time $(R_S + 50\Omega)/50\Omega$, and show that as this speedup is increased, I_{switch} decreases (due to reduction of I_{latch}), resulting in a significantly reduced DE.

To investigate the latched state, we fabricated devices designed to probe the stability of self-heating hotspots as a function of I_0 , L , and R_L . Each device consisted of three sections in series, as shown in Fig. 2 (a): a $3\mu\text{m}$ -long, 100 nm-wide nanowire where the hotspot was nucleated [11]; a wider (200 nm) meandered section acting as an inductance; and a series of nine contact pads interspersed with Ti-film resistors. Also shown are the two electrical probes, which result in the circuit of Fig. 2(b): a high-impedance ($R_p = 20\text{k}\Omega$) 3-point measurement of the nanowire resistance. We varied R_L by touching the probes down to different pads along the line, and L by testing different devices (with different series inductors). We tested 66 devices on three chips, and selected from

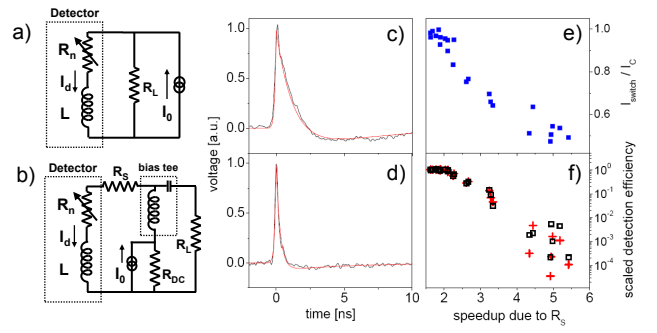


FIG. 1: Figure 1:(color online) Speedup and latching of nanowire detectors with increased load impedance. (a) electrical model of detector operation. A hotspot is nucleated by absorption of a photon, producing a resistance R_n in series with the wire's kinetic inductance L . (b) circuit describing experimental configuration for increasing load resistance using a series resistor R_S . (c) and (d) averaged pulse shapes from $3\mu\text{m} \times 3.3\mu\text{m}$ detectors with $L \sim 50$ nH for $R_S = 0$ and $R_S = 250\Omega$; red solid lines are predictions with no free parameters. (e) switching current $I_{switch} \equiv \min(I_c, I_{latch})$ vs. speedup $50\Omega/(R_S + 50\Omega)$. For small R_S , $I_{switch} = I_c$ but as R_S is increased, I_{latch} decreases, becoming less than I_c . (f) DE at $I_0 = 0.975 I_{switch}$ vs. speedup (open squares). Also shown (crosses) are the expected DEs assuming that latching affects DE simply by limiting I_0 (obtained from DE vs. I_0 at $R_S = 0$).

these only unconstricted [12] wires with nearly identical linewidths (the observed I_c of devices used here were within $\sim 10\%$ of each other - typically $22\text{-}24\ \mu\text{A}$), spanning the range: $R_L = 20 - 1000\Omega$ and $L = 6 - 600$ nH.

For each L and R_L , we acquired a DC I-V curve like those shown in Figs. 2(c),(d), sweeping I_0 downward starting from high values where the hotspot was stable [14]. All curves exhibit a step in voltage which can be identified as I_{latch} . For smaller R_L , where I_{latch} is large, I_c can be identified as the point where an onset of resistance occurs common to several curves; this onset is more gradual with I_0 rather than sudden as at I_{latch} . These features can be understood by examining figs. 2(e) and (f), which show I_d and R_n inferred from the data of fig. 2(d). Above the discontinuous jump in current at I_{latch} , I_d is fixed at I_{ss} (independent of I_0 and R_L) indicating the latched state. For smaller τ_e , $I_{latch} < I_c$, so only I_{latch} is observed [18]. When τ_e is large enough that $I_{latch} > I_c$, an intermediate region appears where the resistance increases continuously with I_0 ; this arises from relaxation oscillations [9, 16], as indicated in the figure: the device cannot superconduct when $I_0 > I_c$, but neither can a stable hotspot be formed when $I_0 < I_{latch}$, so instead current oscillates back and forth between the device and the load, producing a periodic pulse train with a frequency that increases as I_0 is increased [17]. The average resistance increases with this frequency, producing the observed continuous decrease in I_d .

Figure 3 shows the measured I_{latch} as a function of R_L and L , which can be thought of as defining the boundary

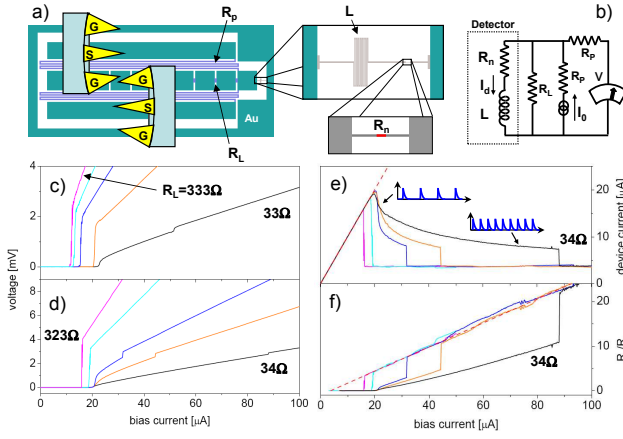


FIG. 2: Figure 2: (color online) Hotspot stability measurements. (a) device schematic; two ground-signal-ground probes simultaneously perform a high-impedance 3-point measurement of the hotspot resistance, with R_L determined by probe position. (b) equivalent electrical circuit. (c) and (d) example V-I curves, with $L = 60$ nH and $L = 605$ nH, respectively; (e) and (f) inferred I_d and R_n/R_L for the data shown in (d). In (e) the relaxation oscillations in the region $I_c < I_0 < I_{\text{latch}}$ are shown schematically. Dashed lines show (e) $I_d = I_0$ and (f) $R_{ss} = R_L(I_0/I_{ss} - 1)$.

between stable and unstable hotspots. Our simple model described above predicts: $\tau_e/\tau_{th} \propto (I_{\text{latch}}/I_{ss})^2$, a line of slope 1 in the figure (indicated by the dashed line). The data do approach this line, though only in the $\tau_e \gg \tau_{th}$ limit. This is consistent with the assumption of constant (or slowly varying) I_d under which eq. 1 was derived. As τ_e/τ_{th} is decreased, the data trend downward, away from this line, and I_{latch}/I_{ss} becomes *almost independent* of τ_e/τ_{th} ; this implies a minimum I_{latch}/I_{ss} , or equivalently, a minimum R_{ss}/R_L , below which the hotspot is *always* unstable. This is shown in the inset: the measured minimum stable R_{ss} is always greater than $\sim R_L$.

The crossover to this behavior can be explained in terms of a timescale τ_a over which the temperature profile of the hotspot stabilizes into the steady-state form which yields eq. 1. For power density variations occurring faster than this, the NS boundaries do not have time to start moving, resulting instead in a temperature deviation ΔT . Since the NS boundary occurs at $T \approx T_c$, where ρ_n is temperature-dependent (defined by $d\rho/dT \equiv \beta > 0$), this changes R_n , giving a second, parallel electrothermal feedback path which dominates for frequencies $\omega \gg \tau_a^{-1}$. We can describe this by replacing eq. 1 with:

$$\frac{\gamma\rho_n}{2} \left(\tau_a \frac{d^2 l}{dt^2} + \frac{dl}{dt} \right) = I_d^2 \rho(\Delta T) - I_{ss}^2 \rho_n \quad (2)$$

$$c \frac{d\Delta T}{dt} = \frac{\gamma\rho_n\tau_a}{2} \frac{d^2 l}{dt^2} - h\Delta T \quad (3)$$

Here, l is the hotspot length, $\rho(\Delta T)$ is the resistance per unit length, and $R_n = \rho(\Delta T)l$. In eq. 2, τ_a is the charac-

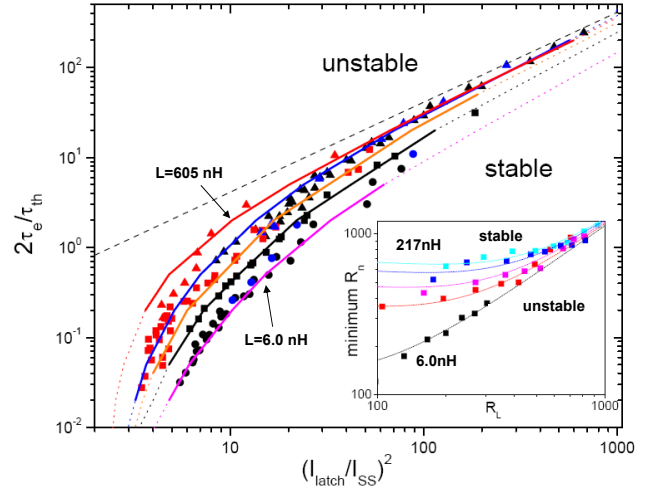


FIG. 3: Figure 3: (color online) Summary of hotspot stability results. Data are shown from 3 different chips (indicated by different colors). Circles, squares, and triangles are data for $L = 6$ -12, 15-60, and 120-600 nH, respectively. In the $\tau_e \gg \tau_a$ limit (where NS domain-wall motion dominates the electrothermal feedback), the data approach the dashed line, which is the prediction based on eq. 1, discussed in the text. For $\tau_e \ll \tau_{th}$ the NS domain walls are effectively fixed and the temperature feedback dominates. In this regime the feedback is always unstable when $R_{ss} \sim > R_L$ (or equivalently, $I_0 \sim < 2I_{ss}$), as shown in the inset. The solid curves are obtained from eq. 8 assuming a phase margin of 30 degrees; each curve corresponds to a fixed L in the set (6,15,30,60,600) nH and spans the range of R_L in the data. The dotted lines extend these predictions over a wider range of R_L .

teristic time over which $dl/dt = 2v_{ns}$ adapts to changes in power density: for slow timescales $dt \gg \tau_a$, $\tau_a d^2 l/dt^2 \ll dl/dt$ and eq. 2 reduces to eq. 1 (with $\rho = \rho_n$). For faster timescales, $\tau_a d^2 l/dt^2$ becomes appreciable, and acts as a source term for temperature deviations in eq. 3. When $dt \ll \tau_a$, $\tau_a d^2 l/dt^2 \gg dl/dt$ and eqs. 2 and 3 can be combined to give: $cd\Delta T/dt \approx I_d^2 \rho - I_{ss}^2 \rho_n - h\Delta T$ [19]. In this limit, if $R_L \sim R_{ss}$ the bias circuit including R_L begins to look like a current source, which then results in positive feedback: a current change produces a temperature and resistance change of the same sign. Therefore, the hotspot is always unstable when $R_{ss} < R_L$.

Expressing eqs. 2 and 3 in dimensionless units ($i \equiv I_d/I_0$, $r \equiv R_n/R_L$, $\lambda \equiv l\beta T_c/R_L$, $\theta \equiv T/T_c$), and expanding to first order in small deviations from steady state, we obtain:

$$\delta i' = -(i_0 \delta i + i_0^{-1} \delta r) \quad (4)$$

$$\delta r = \eta(i_0 - 1) \delta \theta + \eta^{-1} \delta \lambda \quad (5)$$

$$\frac{\tau_a}{\tau_e} \delta \lambda'' + \delta \lambda' = 2\eta^2 \frac{\tau_e}{\tau_{th}} (\delta \theta + 2i_0 \eta^{-1} \delta i) \quad (6)$$

$$\delta \theta' = \frac{\Theta \tau_{th} \tau_a}{\eta \tau_e \tau_c} \delta \lambda'' - \frac{\tau_e}{\tau_c} \delta \theta \quad (7)$$

Here, the prime denotes differentiation with respect to t/τ_e , $i_0 \equiv I_0/I_{ss}$, $\Theta \equiv (T_c - T_0)/T_c$, $\eta \equiv \beta T_c/\rho_n$ characterizes the resistive transition slope, and $\tau_c \equiv c/h$ is a cooling time constant. When $\tau_e \gg \tau_{th}, \tau_a$, the system reduces to: $\delta i'' + i_0 \delta i' - 4\tau_e/\tau_{th} \approx 0$, which has damping coefficient $\zeta = i_0(4\sqrt{\tau_e/\tau_{th}})^{-1}$, as above. In the opposite limit, where $\tau_e \ll \tau_{th}, \tau_a$, we obtain: $\delta i'' + i_0 \delta i' + (2\eta\Theta\tau_e/\tau_c)(i_0 - 2) \approx 0$. In agreement with our argument above, the oscillation frequency becomes negative for $R_{ss} < R_L$ ($I_0 < 2I_{ss}$).

We characterize the stability of the system of eqs. 4-7 using its ‘‘open loop’’ gain A_{ol} : we assume a small oscillatory perturbation by replacing δr in eq. 4 with $\Delta r e^{j\omega t}$, and responses $(\delta i, \delta \theta, \delta \lambda, \delta r)e^{j\omega t}$. Solving for $A_{ol} \equiv \delta r/\Delta r$, we obtain:

$$A_{ol} = \frac{4\frac{\tau_e}{\tau_{th}}(1 + j\omega\frac{\tau_c}{\tau_e}) - 4\eta\Theta\omega^2(i_0 - 1)\frac{\tau_a}{\tau_e}}{j\omega i_0(1 + \frac{j\omega}{i_0}) \left[2j\omega\eta\Theta\frac{\tau_a}{\tau_e} - (1 + j\omega\frac{\tau_c}{\tau_e})(1 + j\omega\frac{\tau_a}{\tau_e}) \right]} \quad (8)$$

The stability of the system can then be quantified by the phase margin: $\pi + \arg[A_{ol}(\omega_0)]$, where ω_0 is the unity gain ($|A_{ol}| = 1$) frequency. In the extreme case, when the phase margin is zero ($\arg[A_{ol}(\omega_0)] = -\pi$), the feedback is positive. The solid lines in Fig. 3 show our best fit to the data. Note that although the stability is determined only by τ_e/τ_{th} and i_0 in the two extreme limits (not visible in the figure), in the intermediate region of interest here this is not the case, so several curves are shown. Each solid curve segment corresponds to a single L , over the range of R_L tested; the dotted lines continue these curves for a wider range of R_L . The data are grouped into

three inductance ranges: 6-12, 15-60, and 120-600 nH, indicated by circles, squares, and triangles, respectively. We used fixed values $\Theta = 0.8$, $\eta = 6.5$, which are based on independent measurements, and fitted $\tau_a = 1.9$ ns, and $\tau_c = 7.7$ ns to all data. Separate values of $\rho_n v_0$ were fitted to data from each of the three chips, differing at most by a factor of ~ 2 . These fitted values were $\rho_n v_0 \sim 1 \times 10^{11} \Omega/s$; since $\rho_n \sim 10^9 \Omega/m$, this gives $v_0 \sim 100$ m/s, a reasonable value.

A natural question to ask in light of this analysis is whether it suggests a method for speeding up these devices. The most obvious way would be to increase the heat transfer coefficient h , which increases both I_{ss} and v_0 , moving the wire further into the unstable region, and allowing its speed to be increased further without latching. However, at present it is unknown how much h can be increased before the DE begins to suffer. At some point, the photon-generated hotspot will disappear too quickly for the wire to respond in the desired fashion. In any case, experiments like those described here will be a useful measurement tool in future work for understanding the impact of changes in the material and/or substrate on the thermal coupling and electrothermal feedback.

We acknowledge helpful discussions with Sae Woo Nam, Aaron Miller, Enectalí Figueroa-Feliciano, and Jeremy Sage.

This work is sponsored by the United States Air Force under Contract #FA8721-05-C-0002. Opinions, interpretations, recommendations and conclusions are those of the authors and are not necessarily endorsed by the United States Government.

-
- [1] G. Goltsman, O. Minaeva, A. Korneev, M. Tarkhov, I. Rubtsova, A. Divochiy, I. Milostnaya, G. Chulkova, N. Kaurova, B. Voronov, D. Pan, J. Kitaygorsky, A. Cross, A. Pearlman, I. Komissarov, W. Slysz, M. Wegrzecki, P. Grabiec, and R. Sobolewski, *IEEE Trans. Appl. Supercond.* **17**, p.246 (2007); F. Marsili, D. Bitauld, A. Gaggero, R. Leoni, F. Mattioli, S. Hold, M. Benkahoul, F. Levy, A. Fiore, *European Conference on Lasers and Electro-Optics and the International Quantum Electronics Conference*, 2007, p. 816; S. N. Dorenbos, E. M. Reiger, U. Perinetti, V. Zwiller, T. Zijlstra, and T. M. Klapwijk, *Appl. Phys. Lett.* **93**, p. 131101 (2008); A.D. Semenov, P. Haas, B. Günther, H.-W. Hübers, K. Ilin, M. Siegel, A. Kirste, J. Beyer, D. Drung, T. Schurig, and A. Smirnov, *Supercond. Sci. Technol.* **20** p. 919924 (2007); S. Miki, M. Fujiwara, M. Sasaki, B. Baek, A.J. Miller, R.H. Hadfield, S.W. Nam, and Z. Wang *Appl. Phys. Lett.*, **92**, p. 061116 (2008); J.A. Stern and W.H. Farr, *IEEE Trans. Appl. Supercond.*, **17**, p. 306-9 (2007).
- [2] A.J. Kerman, E.A. Dauler, W.E. Keicher, J.K.W. Yang, K.K. Berggren, G.N. Gol'tsman, and B.M. Voronov, *Appl. Phys. Lett.* **88**, p. 111116 (2006).
- [3] K.M. Rosfjord, J.K.W. Yang, E.A. Dauler, A.J. Kerman, V. Anant, B.M. Voronov, G.N. Gol'tsman, and K.K. Berggren, *Opt. Express.* **14**, pp. 527-534 (2006).
- [4] E.A. Dauler, A.J. Kerman, B.S. Robinson, J.K.W. Yang, B. Voronov, G. Gol'tsman, S.A. Hamilton, and K.K. Berggren, e-print physics/0805.2397.
- [5] D. Rosenberg, S.W. Nam, P.A. Hiskett, C.G. Peterson, R.J. Hughes, J.E. Nordholt, A.E. Lita, A.J. Miller, *Appl. Phys. Lett.* **88**, p. 21108, (2006); H. Takesue, S.W. Nam, Q. Zhang, R.H. Hadfield, T. Honjo, K. Tamaki, Y. Yamamoto, *Nature Photonics* **1**, p. 343 (2007).
- [6] B.S. Robinson, A.J. Kerman, E.A. Dauler, D.M. Borson, S.A. Hamilton, J.K.W. Yang, V. Anant, and K.K. Berggren *Proc. SPIE* **6709**, p. 67090Z (2007).
- [7] An alternative has recently been demonstrated involving many parallel nanowires [A. Korneev, A. Divochiy, M. Tarkhov, O. Minaeva, V. Seleznev, N. Kaurova, B. Voronov, O. Okunev, G. Chulkova, I. Milostnaya, K. Smirnov, and G. Goltsman, *J. Phys. Conf. Series* **97** p. 012307 (2008)], however, it is as yet unknown whether this method can also achieve the high detection efficiency and low jitter of state-of-the art conventional devices.
- [8] J.K.W. Yang, A.J. Kerman, E.A. Dauler, V. Anant, K.M. Rosfjord, and K.K. Berggren *IEEE Trans. Appl. Supercond.* **17**, p. 581 (2007).
- [9] A.V. Gurevich and R.G. Mints, *Rev. Mod. Phys.* **59**,

- p.941 (1987), and references therein.
- [10] This description is further simplified by the fact that near the NS boundary all material properties can be approximated by their values at T_c .
- [11] The sheet resistance of the NbN is $R_{\square} \approx 500\Omega$, and that the longest hotspot measured in this work is ~ 300 nm.
- [12] A.J. Kerman, E.A. Dauler, J.K.W. Yang, K.M. Rosfjord, V. Anant, K.K. Berggren, G.N. Gol'tsman, and B.M. Voronov, *Appl. Phys. Lett.* **90**, p. 101110 (2007).
- [13] We have focused on the impact of electrothermal feedback on reset time, but it may also influence the timing jitter since it opposes the fast, initial growth of the normal domain that produces the sharp leading-edge of the output pulses.
- [14] The results are almost identical when sweeping I_0 upward, since the dark counts of the device allow it to lock into the latched state if it is stable.
- [15] R.J. Molnar, E.A. Dauler, A.J. Kerman, and K.K. Berggren, to be published.
- [16] R.H. Hadfield, A.J. Miller, S.W. Nam, R.L. Kautz, and R.E. Schwall, *Appl. Phys. Lett.* **87**, p. 203505 (2005).
- [17] In typical experiments, the DC impedance to ground R_{DC} is determined by the I_0 source behind a bias tee, [Fig. 1(b) with $R_S = 0$]. When I_c is exceeded, the detector oscillates (if $I_{\text{latch}} > I_c$), for the time constant of the bias tee, after which it senses the larger R_{DC} and latches. The absence of this burst of pulses is a signature for $I_{\text{latch}} < I_c$.
- [18] When $I_{\text{latch}} < I_c$, I_{latch} is equivalent to what is often called the “retrapping” current in superconducting devices exhibiting self-heating.
- [19] This situation is identical to that encountered in superconducting transition-edge sensors (see, e.g.: K.D. Irwin, G.C. Hilton, D.A. Wollman, and J.M. Martinis, *J. Appl. Phys.* **83**, p.3978 (1998)).